Diffusion Basis Spectrum Imaging Measures Anti-Inflammatory and Neuroprotective Effects of Fingolimod on Murine Optic Neuritis

Ruimeng Yang
Guangzhou First People's Hospital https://orcid.org/0000-0003-2768-9429
Tsen-Hsuan Lin
Washington University in St Louis
Jie Zhan
Washington University in St Louis
Shengsheng Lai
Guangdong Food and Drug Vocational College
Chunyu Song
Washington University School of Medicine in Saint Louis: Washington University in St Louis School of Medicine
Peng Sun
Washington University School of Medicine in Saint Louis: Washington University in St Louis School of Medicine
Zezhong Ye
Washington University School of Medicine in Saint Louis: Washington University in St Louis School of Medicine
Michael Wallendorf
Washington University School of Medicine in Saint Louis: Washington University in St Louis School of Medicine
Ajit George
Washington University School of Medicine in Saint Louis: Washington University in St Louis School of Medicine
Anne. H Cross
Washington University School of Medicine in Saint Louis: Washington University in St Louis School of Medicine
Sheng-Kwei Song (ssong@wustl.edu)
Washington University in St Louis https://orcid.org/0000-0003-1050-7449

Research

Keywords: optic neuritis, demyelination, magnetic resonance imaging, diffusion weighted imaging, diffusion tensor imaging, diffusion basis spectrum imaging

DOI: https://doi.org/10.21203/rs.3.rs-141077/v1

Abstract

Background A readily implemented noninvasive imaging modality for evaluating underlying disease pathology of optic neuritis (ON) and effectiveness of therapeutics in people with CNS demyelinating diseases is currently lacking. This study aims to prospectively determine whether diffusion basis spectrum imaging (DBSI) detects, differentiates and quantitates coexisting inflammation, demyelination, axonal injury and axon loss in mice with ON due to experimental autoimmune encephalomyelitis (EAE), and to determine if DBSI accurately measures effects of fingolimod on underlying pathology.

Methods EAE was induced in 7-week-old C57BL/6 female mice. Visual acuity (VA) was assessed daily to detect onset of ON (VA $\leq$ 0.25 cycle/degree of either eye) after which daily oral treatment with either fingolimod (1 mg/kg) or saline was given for ten weeks. *In vivo* DBSI scans of optic nerves were performed at baseline (before immunization), 2-, 6- and 10-weeks post treatment. DBSI-derived metrics including restricted isotropic diffusion tensor fraction (putatively reflecting cellularity), non-restricted isotropic diffusion tensor fraction (putative reflecting vasogenic edema), DBSI-derived axonal volume, axial diffusivity, $\lambda_{\parallel}$ (putative reflecting axonal integrity), and increased radial diffusivity, $\lambda_{\perp}$ (putatively reflecting demyelination). Mice were killed immediately after the last DBSI scan for immunohistochemical assessment.

Results Optic nerves of fingolimod-treated mice exhibited significantly higher ($p < 0.05$) VA scores than saline-treated group at each time point. During ten-week of treatment, DBSI-derived non-restricted and restricted isotropic diffusion tensor fractions, and axonal volumes were not significantly different ($p > 0.05$) from the baseline values in fingolimod-treated mice, suggesting protection in the fingolimod treated mice. In contrast, in the saline-treated mice, transient DBSI-$\lambda_{\parallel}$ decrease and DBSI-$\lambda_{\perp}$ increase were also detected during Fingolimod treatment. DBSI-derived metrics assessed in vivo significantly correlated ($p < 0.05$) with the corresponding histological markers.

Conclusions DBSI was used to assess changes of the underlying optic nerve pathologies in EAE mice with ON, exhibiting great potential as a noninvasive outcome measure for monitoring disease progression and therapeutic efficacy for MS.

Background

Multiple sclerosis (MS) is an immune-mediated inflammatory demyelinating disease of central nervous system (CNS). Irreversible axonal injury and axon loss are believed to be major causes of permanent neurologic impairments in MS(1, 2). Although early intervention with disease-modifying therapy (DMT) has been shown to decrease the relapse rate and slow short-term disability progression in MS patients(3), it is still uncertain whether it is associated with a lower long-term risk of disability(4, 5). To address this issue, robust markers which can precisely capture and discriminate axonal loss from other underlying pathologies, such as inflammation and demyelination, and monitor intervention response are urgently

needed to help clinicians make more efficient personalized management decision for MS patients and to assess responses to treatments.

Optic neuritis (ON) is a frequent manifestation of MS, and is also frequently encountered on its own, or as part of other diseases such as neuromyelitis optica and myelin oligodendrocyte glycoprotein antibody disease. Conventional T_2-weighted imaging, T_1-weighted gadolinium contrast enhanced imaging, magnetization transfer imaging (MTI), diffusion tensor imaging (DTI) have been widely applied on the evaluation of optic nerve in MS-related ON(6–10). In addition, optic nerve damages in patients with MS have been commonly assessed based on optical coherence tomography (OCT) measured retinal nerve fiber layer thickness change(11).

A lack of pathological specificity of these imaging modalities has contributed to discrepancies between neuroimaging findings and clinical outcomes, commonly known as the clinicoradiological paradox(12–14). This paradox is due to many factors, including the heterogeneous nature of MS in clinical course and underlying pathologies(15, 16). We have developed diffusion basis spectrum imaging (DBSI) and demonstrated its ability to detect and differentiate inflammation, axonal injury, axon loss and demyelination in mice with experimental autoimmune encephalomyelitis (EAE), and autopsied and biopsied specimens from MS patients (2, 17–22).

Therefore, we hypothesized that DBSI, which is pathologically more specific than standard MRI, would be able to assess the efficacy of fingolimod (also known as FTY720, Selleck Chemicals LLC, USA) treatment of ON through longitudinally quantifying the evolution of several coexisting optic nerve pathologies using a preclinical EAE mouse model which has ON.

Methods

Animal Model

Procedures were approved by Washington University Institutional Animal Care and Use Committee. Female C57BL/6 mice at 7 weeks of age were obtained from Jackson Laboratory (Bar Harbor, ME).

Induction of EAE and Visual Acuity (VA) Measurements in Mice

Before immunization, mice were housed under humidity and temperature-controlled conditions with 12-hour dark/light cycle for two weeks. Mice then underwent baseline DBSI of optic nerves. Two weeks after baseline DBSI, mice were immunized with 50 μg myelin oligodendrocyte glycoprotein $(MOG)_{35-55}$ peptide emulsified (1:1) in incomplete Freund's adjuvant (IFA), followed by intravenous Pertussis toxin (300 ng; PTX, List Laboratories, Campbell, CA, USA) injection on the day of MOG_{35-55} immunization and two days later to induce EAE (Fig. 1A).

The VA of mice was measured as previous described using the Virtual Optomotry System (Optomotry, Cerebral Mechanics, Inc., Lethbridge, Canada). Before immunization, normal VA was confirmed for each eye (VA = 0.34 ± 0.04 c/d, n = 34 eyes from 17 mice) at baseline due to unrelated factors. After immunization, blinded VA measurement was performed daily before the onset of ON (9–22 days post-immunization) which was defined as VA ≤ 0.25 c/d in our previous study(23–25), and then weekly till the end of the study (Fig. 1B).

Fingolimod Treatment

Starting on the first day of onset of ON, mice were alternately assigned to either receive daily gavage of fingolimod (n = 9 mice, 1 mg/kg, Cat No. S5002, Selleck Chemicals LLC, USA) or the same volume of saline (n = 9 mice) for 10 consecutive weeks. Mice were alternately assigned to receive fingolimod or saline until the 9th pair. The final number in fingolimod- and saline-treated group was 8 and 9 EAE mice, respectively due to the lack of VA impairment or clinical signs during the course of assessment of the last EAE mouse assigned to fingolimod treatment.

In Vivo Diffusion Basis Spectrum Imaging (DBSI)

In vivo DBSI was performed two weeks before immunization (baseline DBSI), and then at two, six and ten weeks after initiation of fingolimod treatment. DBSI were performed on a 4.7-T small-animal MRI scanner (Agilent/Varian, Santa Clara, CA) equipped with an Agilent/Magnex HD imaging gradient coil (Magnex/Agilent, Oxford, UK). Mice were anesthetized with isoflurane/O_2 [2% (vol/vol) for induction followed by 0.7–0.8% for maintenance] throughout the imaging experiment. Body temperature was maintained at 37°C with a circulating warm water pad. A diffusion weighted mid-sagittal image was acquired to localize mouse optic nerves, followed by an oblique image plan perpendicular to the optic nerve to obtain the final image view using a multi-echo spin-echo diffusion-weighting sequence. The final diffusion-weighted MRI for DBSI analysis employed a 25-direction diffusion-encoding scheme adding an extra b = 0 data as previously reported(23) with the following acquisition parameters: TR = 1500 ms, TE = 35 ms, NE = 2, inter-echo delay = 20.7 ms, FOV = 22.5 × 22.5 mm^2, matrix size = 192 × 192 (zero-filled to 384 × 384), slice thickness = 0.8 mm, maximal b-value = 2,200 s/mm^2, total scan time = 2 hr. 4 min.

Imaging Analysis

Diffusion-weighted MR images were analyzed by DBSI multi-tensor model software developed in-house with MATLAB (The Mathworks, Natick, MA, USA) as described previously(17, 20). Regions of interest (ROIs) were manually drawn with ImageJ (https://imagej.nih.gov/ij/, NIH, Bethesda, MA, US) on the diffusion-weighted image (DWI, with the diffusion-weighting direction perpendicular to the optic nerve) avoiding the inclusion of nerve-cerebrospinal fluid interface to minimize partial volume effects. ROI-based analysis was performed to assess DBSI metrics. A separate, larger ROI encompassing the whole optic nerve and surrounding cerebrospinal fluid was drawn on the same cross-sectional images for assessing DBSI-derived axonal volume (= an fictitious volume for the purpose of quantitating axonal loss = optic

nerve volume assessed by the entire ROI on DWI × DBSI fiber fraction, the total diffusion signal associated with axonal fiber bundle).

Histology Analysis

After the last DBSI scan, mice were killed and the optic nerves were collected and embedded in 2% agar gel(26), followed by paraffin embedding of the agar block. The paraffin blocks were cut in the axial plane at a thickness of 5-μm for immunohistochemistry (IHC) staining, including SMI-31, SMI-312, MBP, and DAPI.

Statistical Analysis

Data were presented as mean ± standard deviation. VA and MRI measurements were performed on each eye at baseline, end of two-, six- and ten-week treatment. Data were analyzed with a mixed random effects repeated measures model with side, time, treatment, and time by treatment interaction as fixed effects. Two samples student's t-test was used to compare two different test groups. The correlation of histology data (SMI-31, SMI-312, MBP and DAPI) and DBSI metrics at 10 weeks after treatment were analyzed by Pearson correlation analysis. A difference of $p < 0.05$ was considered significant.

Results

Visual acuity (VA) in Fingolimod-treated mice was better than that in saline-treated mice

There was no VA difference between fingolimod-treated (0.34 ± 0.03 c/d, n = 16 eyes, from 8 EAE mice) and saline-treated groups (0.36 ± 0.04 c/d, n = 18 eyes, from 9 EAE mice) at baseline before treatment. Over the treatment period, the VA of fingolimod-treated mice was significantly better than saline-treated mice from 3 days to 10 weeks after treatment onset ($p < 0.05$, Fig. 1B).

DBSI detected the reduced inflammation in fingolimod-treated optic nerves

Representative DBSI non-restricted isotropic fraction (putatively reflecting vasogenic edema) and restricted isotropic fraction (putatively reflecting cellularity) maps of optic nerves were presented to demonstrate the evolution of these markers at baseline (before immunization), 2, 6, and 10 weeks after treatment (Fig. 2A).

In the group of saline-treated mice with ON, non-restricted isotropic fraction of optic nerves significantly increased from baseline by 133% ($p = 0.020$), 198% ($p = 0.001$), and 229% ($p < 0.001$) at 2, 6, and 10 weeks after treatment, respectively (Fig. 2B). Restricted isotropic fraction of optic nerves significantly increased from the baseline by 201% ($p < 0.001$), 98% ($p = 0.070$), and 164% ($p = 0.002$) at 2, 6, and 10 weeks after placebo treatment, respectively (Fig. 2C). In the fingolimod treatment group, non-restricted isotropic fraction increased from baseline by 21% ($p = 0.740$), 48% ($p = 0.440$), and 63% ($p = 0.320$) at 2, 6,

and 10 weeks after treatment (Fig. 2B), while restricted isotropic fraction increased from baseline by 72% ($p = 0.180$), 28% ($p = 0.590$), and 51% ($p = 0.340$) at 2, 6, and 10 weeks (Fig. 2C).

In comparison to the saline-treated group, the fingolimod-treated mice exhibited significantly lower non-restricted isotropic fraction at 2 (60% lower, $p = 0.070$), 6 (62% lower, $p = 0.020$) and 10 weeks (63% lower, $p = 0.010$) after treatment (Fig. 2B). Although the increase in restricted isotropic fraction was numerically greater for the placebo group, differences between the two treatment groups were not statistically significant.

DBSI detected reduced axon loss in Fingolimod-treated optic nerves

Representative fiber fraction (the total diffusion signal from anisotropic axonal fiber bundles) maps of optic nerves at baseline, 2, 6, and 10 weeks after treatment were presented to demonstrate the evolution of fiber fraction (Fig. 3A).

In the saline-treated group, DBSI fiber fraction (putative marker of apparent axonal density) of the optic nerves decreased by 10% ($p = 0.140$), 24% ($p = 0.002$) and 25% ($p = 0.003$) at 2, 6, and 10 weeks, respectively, when compared to baseline before immunization (Fig. 3B). DWI-derived volumes of optic nerves decreased by 23% ($p = 0.004$), 37% ($p < 0.001$) and 25% ($p = 0.002$) at 2, 6, and 10 weeks, respectively, from baseline before immunization (Fig. 3C). DBSI-derived axonal volume (putative marker of axonal content) decreased by 28% ($p = 0.006$), 45% ($p < 0.001$), and 36% ($p < 0.001$) at 2, 6, and 10 weeks, respectively, when compared to baseline before immunization (Fig. 3D). In the fingolimod-treated group, no significant difference from baseline was observed for DBSI fiber fraction, DWI-derived optic nerve volume, or DBSI axonal volume at any time point after treatment.

Compared to saline-treated mice, the fingolimod-treated group exhibited significantly higher DBSI fiber fraction at 6 weeks (38% higher, $p = 0.020$) and 10 weeks (Fig. 3B, 33% higher, $p = 0.030$), with significantly lower DWI-derived optic nerve volumes at 6 weeks (35% higher, $p = 0.02$) and at 10 weeks (39% higher, $p = 0.005$, Fig. 3C). DBSI-derived axonal volumes in the fingolimod-treated optic nerves were higher than for saline-treated optic nerves at 2 weeks (25% higher, $p = 0.400$), 6 weeks (62% higher, $p = 0.020$) and at 10 weeks (64% higher, $p = 0.007$) after treatment commencement (Fig. 3D).

DBSI detection of diminished injury to residual axons in Fingolimod-treated optic nerves

Figure 4A shows representative DBSI axial diffusivity ($\lambda_{\parallel}$) and radial diffusivity ($\lambda_{\perp}$) maps at baseline, 2, 6, and 10 weeks after treatment for each group. Compared to baseline, for saline-treated mice DBSI $\lambda_{\parallel}$ significantly decreased by 17% ($p < 0.001$), 14% ($p < 0.001$), and 12% ($p = 0.001$) at 2, 6, and 10 weeks (Fig. 4B), while DBSI $\lambda_{\perp}$ significantly increased by 45% ($p = 0.015$), 62% ($p = 0.001$) and 75% ($p < 0.001$) at 2, 6, and 10 weeks (Fig. 4C), respectively. In the fingolimod treatment group, DBSI $\lambda_{\parallel}$ decreased by 7% ($p =$

0.040), 7% ($p = 0.033$), 3% ($p = 0.330$) at 2, 6, 10 weeks (Fig. 4B), while DBSI $\lambda_{\perp}$ increased from baseline by 14% ($p = 0.400$), 15% ($p = 0.400$) and 9% ($p = 0.600$) at 2, 6 and 10 weeks after treatment (Fig. 4C).

Compared the difference between groups (saline vs. fingolimod), fingolimod-treated group showed no significant differences on DBSI $\lambda_{\parallel}$ for all the time points while DBSI $\lambda_{\perp}$ decreased by 38% at 10 weeks ($p = 0.010$, Fig. 4C).

Immunohistochemistry (IHC) staining of optic nerves

Mice were euthanized at the end of the treatment period for histologic assessment of the optic nerves. IHC staining of total neurofilaments (SMI-312, stains both injured and intact axons), phosphorylated neurofilaments (SMI-31, stains intact axons), and myelin basic protein (MBP, stains myelin) revealed that the saline-treated group exhibited less staining for SMI-312 (Fig. 5A), MBP (Fig. 5D), and SMI-31 (Fig. 5G), when compared to Fingolimod-treated group (Fig. 5B, E, H). The apparent optic nerve sizes of saline-treated group were smaller than those of Fingolimod-treated group (Figs. 5A - I). However, compared to one representative wildtype (WT) optic nerves (10-week-old C57BL/6 female mouse optic nerve), fingolimod-treated group showed enlarged staining spots (Fig. 5b, e, h; blue arrows), suggesting swollen axons or myelin debris aggregation. Moreover, increased positive DAPI staining areas (cell nuclei) were also seen in both saline and Fingolimod treatment groups compared to WT optic nerve, suggesting increased cellularity (Figs. 5J, K).

DBSI $\lambda_{\parallel}$, DBSI $\lambda_{\perp}$, DBSI-derived axon volume and DBSI restricted fraction correlated well with SMI-31 area fraction ($y = 1.7475x + 1.4709$, slope of standard error = 0.4246, Fig. 6A), MBP area fraction ($y = -0.7347x + 0.3794$, slope of standard error = 0.1556, Fig. 6B), SMI-312 area fraction ($y = 5.0633x + 0.0303$, slope of standard error = 0.8941, Fig. 6C) and DAPI density ($y = 9.585 \times 10^{-6} x + 0.03$, slope of standard error = 1.506×10^{-6}, Fig; 6D), respectively in the ON-affected optic nerves.

Discussion

Understanding of the evolution of chronic human CNS diseases over time and in response to therapies has been hindered by inability to access CNS specimens to examine longitudinally. In this study, we hypothesized that DBSI is capable to assess the efficacy of fingolimod treatment in an animal model of ON. The optic nerve was chosen for examination because it is a frequent site of inflammatory demyelination in MS and related diseases. Moreover, the volume of the optic nerve can be measured, allowing precise measurement of axonal content, even in the presence of inflammation and edema. The novel findings of this study are that DBSI non-invasively distinguished and quantitated several coexisting CNS pathologies over time to measure axonal loss, and to determine the treatment effects of fingolimod (an FDA-approved oral medication for MS). In comparison to saline treatment, less optic nerve inflammation and greater axonal preservation was observed in the optic nerves of mice treated with fingolimod. Moreover, the study suggested that fingolimod treatment resulted in improved myelin integrity in optic nerves of EAE mice.

Optic neuritis, a common occurrence in people with MS, can lead to irreversible visual impairment(26). Fingolimod is approved for patients with RRMS. However, its neuroprotective effects remain uncertain(28). Rau et al. reported apoptotic cell death of retinal ganglion cells in rats with EAE that were treated with fingolimod, although axonal preservation in optic nerves was seen by histological data(29). An et al. reported axonal preservation in optic nerves by histological validation and moderate visual dysfunction (better than non-treated EAE mice but worse than naïve control mice) by optometry(30). However, both studies could only rely upon end-point histological results at the conclusion of study to evaluate whether fingolimod is axonal protective. In the current study, DBSI detected improved transient inflammation (via the putative inflammatory markers) and axonal pathologies (via putative DBSI axonal injury and loss markers) in fingolimod-treated optic nerves. Results suggest axonal protection of fingolimod could be secondary to reduced inflammation.

Consistent with previous reports(2, 17, 20, 21, 31, 32), we followed individual mice over time using DBSI. We observed that daily oral fingolimod markedly reduced inflammation, evidenced by the decrease in DBSI restricted isotropic fraction (reflecting cellular inflammation) and non-restricted isotropic fraction (reflecting vasogenic edema), in accordance with the action of fingolimod to sequester lymphocytes in secondary lymphoid tissue and thus inhibit lymphocytes from entering the CNS(33). Additionally, we also observed that both decreased $\lambda_{||}$ (putative axonal injury, Fig. 4B) and increased $\lambda_{\perp}$ (putative demyelination, Fig. 4C) were significantly improved in mice treated with fingolimod versus those treated with saline. Mice were euthanized and optic nerves were examined histologically at the conclusion of 10-week treatment. As previously reported (17, 24, 25) DBSI longitudinally monitored disease progression. After 10 weeks of fingolimod therapy, reduced inflammation, less demyelination, and diminished axonal injury of optic nerves was confirmed by IHC, suggesting DBSI is capable of detecting long-term anti-inflammatory and neuroprotective effects with fingolimod treatment. The histological findings were consistent with DBSI-derived putative imaging biomarkers of optic nerve pathologies. Following increased $\lambda_{\perp}$ (demyelination) in optic nerves of EAE mice with ON, we noted the subsequent reduction of DBSI $\lambda_{\perp}$ after 10 weeks of fingolimod but not placebo treatment, suggesting remyelination could have occurred in those mice treated with fingolimod.

Limitations of the current study include that we performed histological validation at the last time point, 10 weeks after treatment commenced. Definitive demonstration of the evolution of the underlying optic nerve pathologies may require further cross-sectional histological validation studies. Second, this proof-of-concept study may be limited due to the small sample size (17 mice divided between fingolimod and saline treatment groups). Although each mouse was imaged 4 times, generating 68 imaging datasets thus increasing the power of the study, the limitation of small number of animals studied needs to be kept in mind when drawing a conclusion. Third, visual function is not specific to optic nerve pathologies since EAE (and MS) can affect other parts of the visual system, such as retinal ganglion cells(34). Damage in regions other than the optic nerves was not taken into consideration in the present study.

Conclusions

Our preclinical study demonstrates that DBSI-based biomarkers reflect underlying pathologic changes and, importantly, therapeutic efficacy of an established treatment. Moreover, the results strongly suggest that DBSI can detect and quantitate remyelination following demyelination. These data support that DBSI, a noninvasive contrast agent-free MR technique, offers new possibilities for precise clinical diagnosis as well as assessing disease evolution and treatment responses in CNS inflammatory demyelinating diseases, such as MS.

Abbreviations

AD
Axial diffusivity; DBSI = Diffusion basis spectrum imaging; DTI = Diffusion tensor imaging; DWI = Diffusion-weighted image; FA = Fraction anisotropy; MS = Multiple sclerosis; RD = Radial diffusivity; WM = White matter

Declarations

Acknowledgements

The authors thank Mr. Bob Mikesell for excellent technical assistance.

Ethics approval and consent to participate

All animal experiments were performed according to protocols approved by the Institutional Animal Care and Use Committee (IACUC) at Washington University and in compliance with the NIH guidelines.

Consent for publication

Not applicable

Availability of data and material

Please contact author for data requests.

Competing interests

Sheng-Kwei Song has a financial [ownership] interest in CancerVision LLC and may financially benefit if the company is successful in marketing its product(s) that is/are related to this research. This activity has been reviewed by Washington University's (WU) Conflicts of Interest Review Committee in accordance with WU's Research Conflicts of Interest Policy. Anne H. Cross has performed paid consulting services for Novartis, Biogen, EMD Serono, Genentech and Roche. The rest of authors have no conflicts of interest to report.

Funding

This study was supported in part by the grants from National Institute of Health R01-NS047592 (S.-K.S.), P01-NS059560 (A.H.C.), National Multiple Sclerosis Society (NMSS) RG 4549A4/1 and 1701-26617 (S.-K.S.), FG-1507-05315 (T.-H.L.), the National Natural Science Foundation of China (81971574), the Natural Science Foundation of Guangdong Province in China (2018A030313282), the Science and Technology Program of Guangzhou in China (202002030268), the Fundamental Research Funds for the Central Universities, SCUT (2018MS23).

Authors' contributions

RMY and THL conducted experiments, analyzed data, and jointly wrote the manuscript. PS, AG and ZZY designed the data processing routine and helped analyzing the DBSI data. MW helped with experiment design and conducted the statistical analyses. JZ, SSL and CYS helped with tissue histological analysis design and evaluation. AHC designed experiments and wrote the manuscript. SKS designed experiments and the data processing software, helped analyzing the data, and significantly contributed to the writing of the manuscript. All authors read and approved the final manuscript.

References

1. Rahim T, Becquart P, Baeva ME, Quandt J. Expression of the neuroprotective protein aryl hydrocarbon receptor nuclear translocator 2 correlates with neuronal stress and disability in models of multiple sclerosis. J Neuroinflammation. 2018;15:270.
2. Sun P, George A, Perantie DC, Trinkaus K, Ye Z, Naismith RT, et al. Diffusion basis spectrum imaging provides insights into MS pathology. Neurol Neuroimmunol Neuroinflamm 2020;7.
3. Montalban X, Gold R, Thompson AJ, Otero-Romero S, Amato MP, Chandraratna D, et al. ECTRIMS/EAN Guideline on the pharmacological treatment of people with multiple sclerosis. Mult Scler. 2018;24:96–120.
4. Torkildsen O, Myhr KM, Bo L. Disease-modifying treatments for multiple sclerosis - a review of approved medications. EUR J NEUROL. 2016;23(Suppl 1):18–27.
5. Kavaliunas A, Manouchehrinia A, Stawiarz L, Ramanujam R, Agholme J, Hedstrom AK, et al. Importance of early treatment initiation in the clinical course of multiple sclerosis. Mult Scler. 2017;23:1233–40.
6. Jackson A, Sheppard S, Laitt RD, Kassner A, Moriarty D. Optic neuritis: MR imaging with combined fat- and water-suppression techniques. RADIOLOGY. 1998;206:57–63.
7. Hickman SJ, Toosy AT, Miszkiel KA, Jones SJ, Altmann DR, MacManus DG, et al. Visual recovery following acute optic neuritis–a clinical, electrophysiological and magnetic resonance imaging study. J NEUROL. 2004;251:996–1005.
8. Hickman SJ, Wheeler-Kingshott CA, Jones SJ, Miszkiel KA, Barker GJ, Plant GT, et al. Optic nerve diffusion measurement from diffusion-weighted imaging in optic neuritis. AJNR Am J Neuroradiol. 2005;26:951–6.

9. Rocca MA, Filippi M. Functional MRI in multiple sclerosis. J NEUROIMAGING. 2007;17(Suppl 1):36S–41S.
10. Chang ST, Xu J, Trinkaus K, Pekmezci M, Arthur SN, Song SK, et al. Optic nerve diffusion tensor imaging parameters and their correlation with optic disc topography and disease severity in adult glaucoma patients and controls. J GLAUCOMA. 2014;23:513–20.
11. Gajamange S, Raffelt D, Dhollander T, Lui E, van der Walt A, Kilpatrick T, et al. Fibre-specific white matter changes in multiple sclerosis patients with optic neuritis. NeuroImage: Clinical. 2018;17:60–8.
12. Barkhof F. The clinico-radiological paradox in multiple sclerosis revisited. CURR OPIN NEUROL. 2002;15:239–45.
13. Davis FA. The clinico-radiological paradox in multiple sclerosis: Novel implications of lesion size. Mult Scler. 2014;20:515–6.
14. Costello F, Coupland S, Hodge W, Lorello GR, Koroluk J, Pan YI, et al. Quantifying axonal loss after optic neuritis with optical coherence tomography. ANN NEUROL. 2006;59:963–9.
15. Scalfari A, Neuhaus A, Degenhardt A, Rice GP, Muraro PA, Daumer M, et al. The natural history of multiple sclerosis: A geographically based study 10: Relapses and long-term disability. BRAIN. 2010;133:1914–29.
16. Leray E, Yaouanq J, Le Page E, Coustans M, Laplaud D, Oger J, et al. Evidence for a two-stage disability progression in multiple sclerosis. BRAIN. 2010;133:1900–13.
17. Lin T, Chiang C, Perez-Torres CJ, Sun P, Wallendorf M, Schmidt RE, et al. Diffusion MRI quantifies early axonal loss in the presence of nerve swelling. J NEUROINFLAMM 2017;14.
18. Ye Z, George A, Wu AT, Niu X, Lin J, Adusumilli G, et al. Deep learning with diffusion basis spectrum imaging for classification of multiple sclerosis lesions. Ann Clin Transl Neurol. 2020;7:695–706.
19. Shirani A, Sun P, Trinkaus K, Perantie DC, George A, Naismith RT, et al. Diffusion basis spectrum imaging for identifying pathologies in MS subtypes. Ann Clin Transl Neurol. 2019;6:2323–7.
20. Wang Y, Wang Q, Haldar JP, Yeh F, Xie M, Sun P, et al. Quantification of increased cellularity during inflammatory demyelination. BRAIN. 2011;134:3587–98.
21. Wang Y, Sun P, Wang Q, Trinkaus K, Schmidt RE, Naismith RT, et al. Differentiation and quantification of inflammation, demyelination and axon injury or loss in multiple sclerosis. BRAIN. 2015;138:1223–38.
22. Wang X, Cusick MF, Wang Y, Sun P, Libbey JE, Trinkaus K, et al. Diffusion basis spectrum imaging detects and distinguishes coexisting subclinical inflammation, demyelination and axonal injury in experimental autoimmune encephalomyelitis mice. NMR BIOMED. 2014;27:843–52.
23. Chiang C, Wang Y, Sun P, Lin T, Trinkaus K, Cross AH, et al. Quantifying white matter tract diffusion parameters in the presence of increased extra-fiber cellularity and vasogenic edema. NEUROIMAGE. 2014;101:310–9.
24. Lin T, Kim JH, Perez-Torres C, Chiang C, Trinkaus K, Cross AH, et al. Axonal transport rate decreased at the onset of optic neuritis in EAE mice. NEUROIMAGE. 2014;100:244–53.

25. Wang X, Li XS, Wang WC. [Transnasal endoscopic optic canal decompression for traumatic optic neuropathy without light reception]. Zhonghua Er Bi Yan Hou Tou Jing Wai Ke Za Zhi. 2007;42:625–6.
26. Blewitt ES, Pogmore T, Talbot IC. Double embedding in agar/paraffin wax as an aid to orientation of mucosal biopsies. J CLIN PATHOL. 1982;35:365.
27. Galetta SL, Villoslada P, Levin N, Shindler K, Ishikawa H, Parr E, et al. Acute optic neuritis: Unmet clinical needs and model for new therapies. Neurol Neuroimmunol Neuroinflamm. 2015;2:e135.
28. Ambrosius B, Pitarokoili K, Schrewe L, Pedreiturria X, Motte J, Gold R. Fingolimod attenuates experimental autoimmune neuritis and contributes to Schwann cell-mediated axonal protection. J Neuroinflammation. 2017;14:92.
29. Rau CR, Hein K, Sattler MB, Kretzschmar B, Hillgruber C, McRae BL, et al. Anti-inflammatory effects of FTY720 do not prevent neuronal cell loss in a rat model of optic neuritis. AM J PATHOL. 2011;178:1770–81.
30. An X, Kezuka T, Usui Y, Matsunaga Y, Matsuda R, Yamakawa N, et al. Suppression of experimental autoimmune optic neuritis by the novel agent fingolimod. J Neuroophthalmol. 2013;33:143–8.
31. Lin TH, Sun P, Hallman M, Hwang FC, Wallendorf M, Ray WZ, et al. Noninvasive quantification of axonal loss in the presence of tissue swelling in traumatic spinal cord injury mice. J Neurotrauma 2019.
32. Redler Y, Levy M. Rodent models of optic neuritis. FRONT NEUROL. 2020;11:580951.
33. Zhang J, Zhang ZG, Li Y, Ding X, Shang X, Lu M, et al. Fingolimod treatment promotes proliferation and differentiation of oligodendrocyte progenitor cells in mice with experimental autoimmune encephalomyelitis. NEUROBIOL DIS. 2015;76:57–66.
34. Shindler KS, Guan Y, Ventura E, Bennett J, Rostami A. Retinal ganglion cell loss induced by acute optic neuritis in a relapsing model of multiple sclerosis. Mult Scler. 2006;12:526–32.

Figures

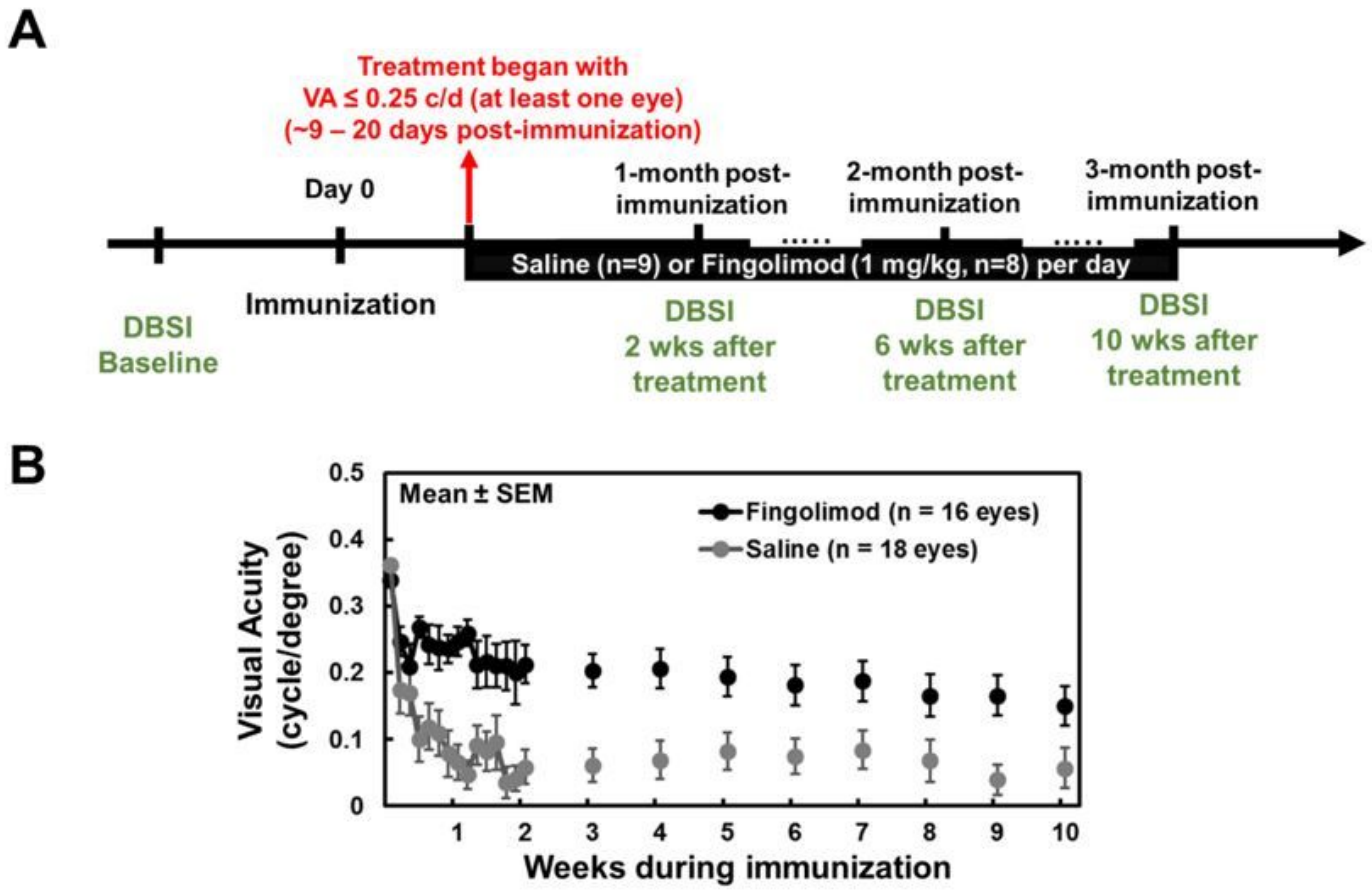

Figure 1

Diagram shows experimental design and visual acuity measurement through the entire experiment. (A) DBSI was performed at two weeks prior to active immunization (as baseline), 2, 6, and 10 weeks after treatment started. Treatment commenced if one eye of visual acuity (VA) ≤ 0.25 cycle/degree (c/d). Daily gavage of either Fingolimod (1 mg/kg) or the equal volume of saline was administrated for 10 weeks. (B) Daily VA was performed at the first two weeks after immunization followed by weekly VA from 3 to 10 weeks. Comparing to VA of saline-treated eyes, VA was significant higher in Fingolimod-treated eyes from Day 3 to ten-week treatment ($p < 0.05$). $\star$ indicates $p < 0.05$, comparing to corresponding saline group

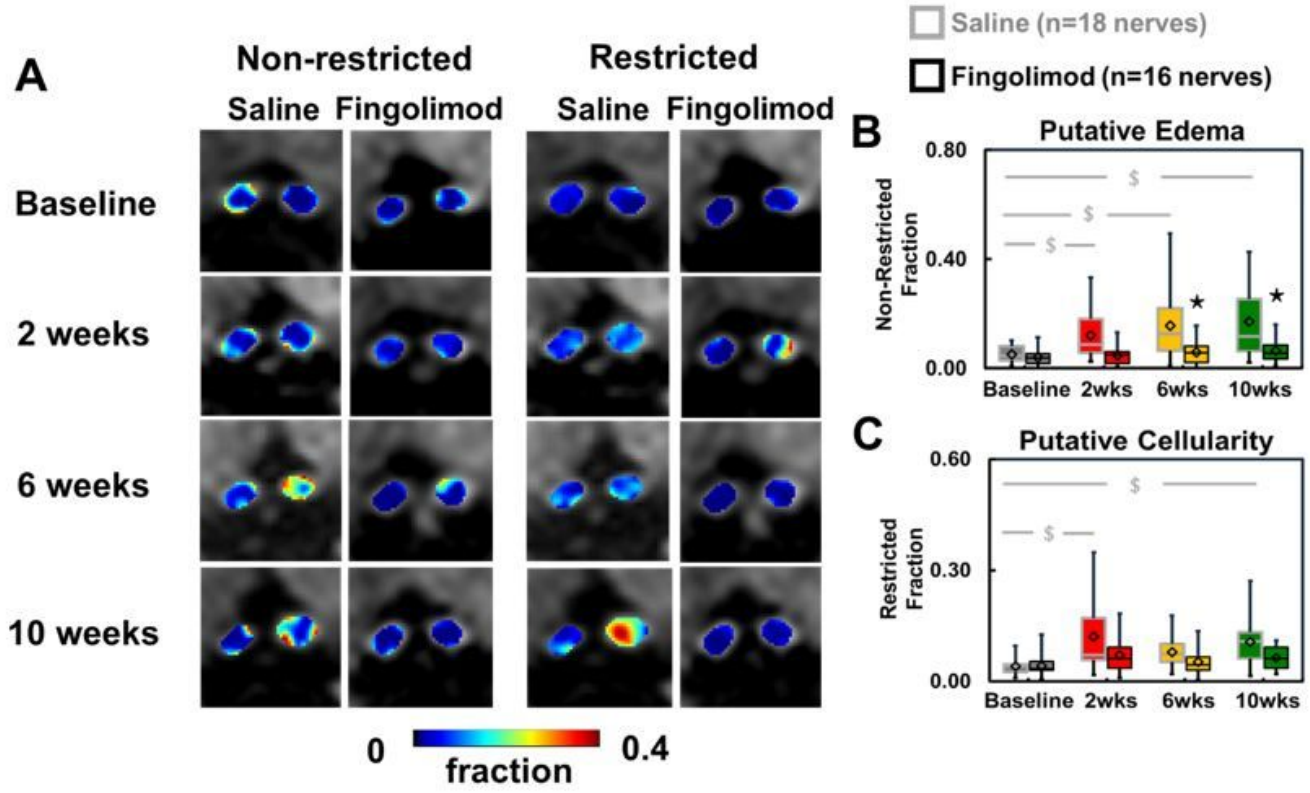

Figure 2

DBSI-derived non-restricted fraction (putative edema) and restricted (putative cellularity) isotropic tensor fraction maps for representative saline- and Fingolimod-treated optic nerves from baseline to 10-week treatment (A). Comparing to baseline, Fingolimod effectively suppressed putative inflammation markers, including non-restricted and restricted fractions, after treatment ($p < 0.05$, B and C). However, significant increase in saline-treated optic nerves from baseline was shown in non-restricted fraction at all time points ($p < 0.05$) and in restricted fraction at 2 and 10 (both $p < 0.05$) but not at 6 ($p = 0.06$) weeks (B and C). Comparing to saline, significantly reduced non-restricted fraction at 6 and 10 weeks ($p < 0.05$) in Fingolimod-treated optic nerves (B). Mild but not significant reduced restricted fraction was shown in Fingolimod-treated optic nerve all the time (C). $\star$ indicates $p < 0.05$, comparing between saline and fingolimod groups $ indicates $p < 0.05$, comparing to its baseline within group

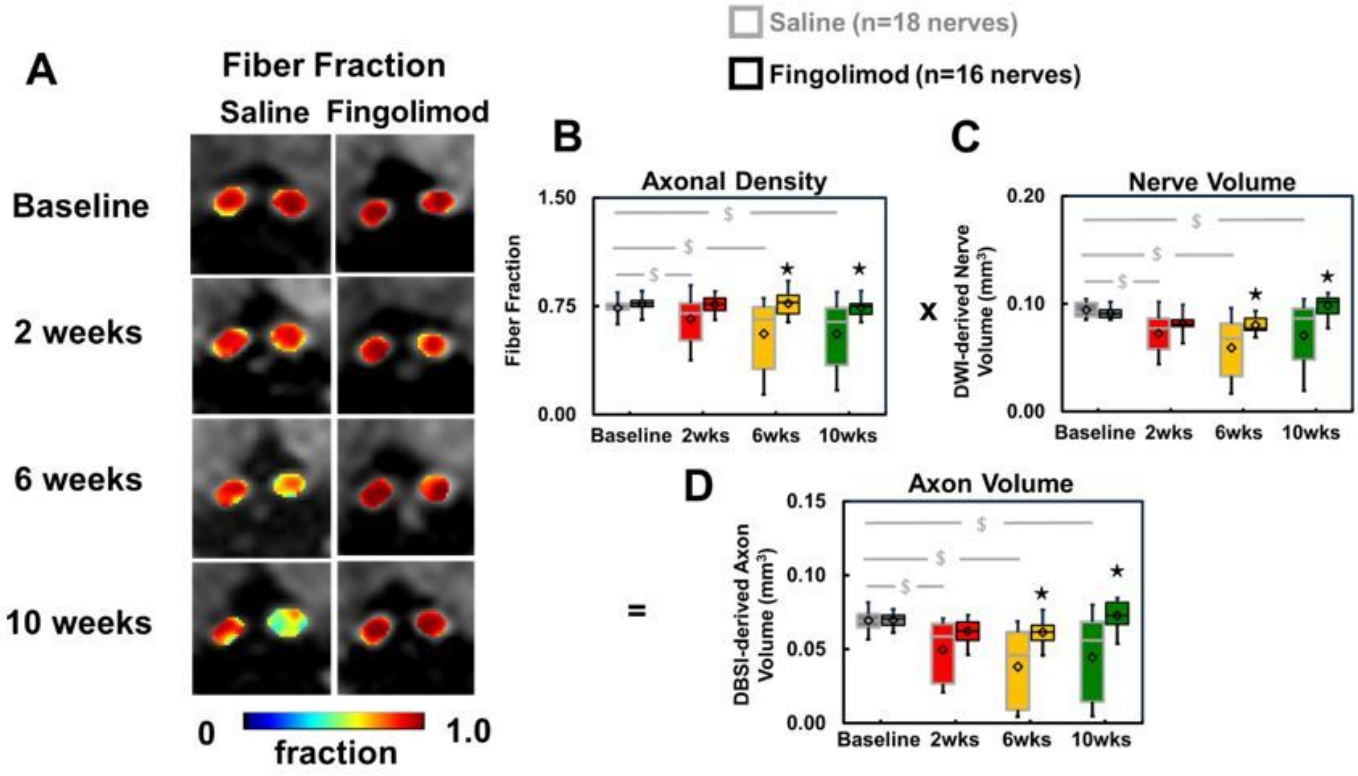

Figure 3

DBSI-derived fiber fraction reflects total signal from anisotropic diffusion tensor components, suggesting axonal fiber density (A, B). Comparing to baseline, significantly decreased fiber fraction was detected at each time point in saline-treated group ($p < 0.05$) but not in Fingolimod-treated optic nerves at all time points (B). Significantly reduced DWI-derived nerve volume was seen in saline-treated optic nerves ($p < 0.05$) but not in Fingolimod-treated group from baseline to the rest of time points (C). To remove the confounding effects from inflammation, DBSI-derived axonal volume (D) was computed multiplying fiber fraction (B) by DWI-derived nerve volume (C) in each individual optic nerve. Comparing to baseline, significantly reduced DBSI-derived axonal volume was shown in saline-treated optic nerves ($p < 0.05$) but not in Fingolimod-treated optic nerves at all time points (D). Comparing to saline group, fingolimod-treated optic nerves showed significantly higher axon volume at all time points (D), suggesting axonal prevention with Fingolimod treatment. ⋆ indicates $p < 0.05$, comparing between saline and fingolimod groups $ indicates $p < 0.05$, comparing to its baseline within group

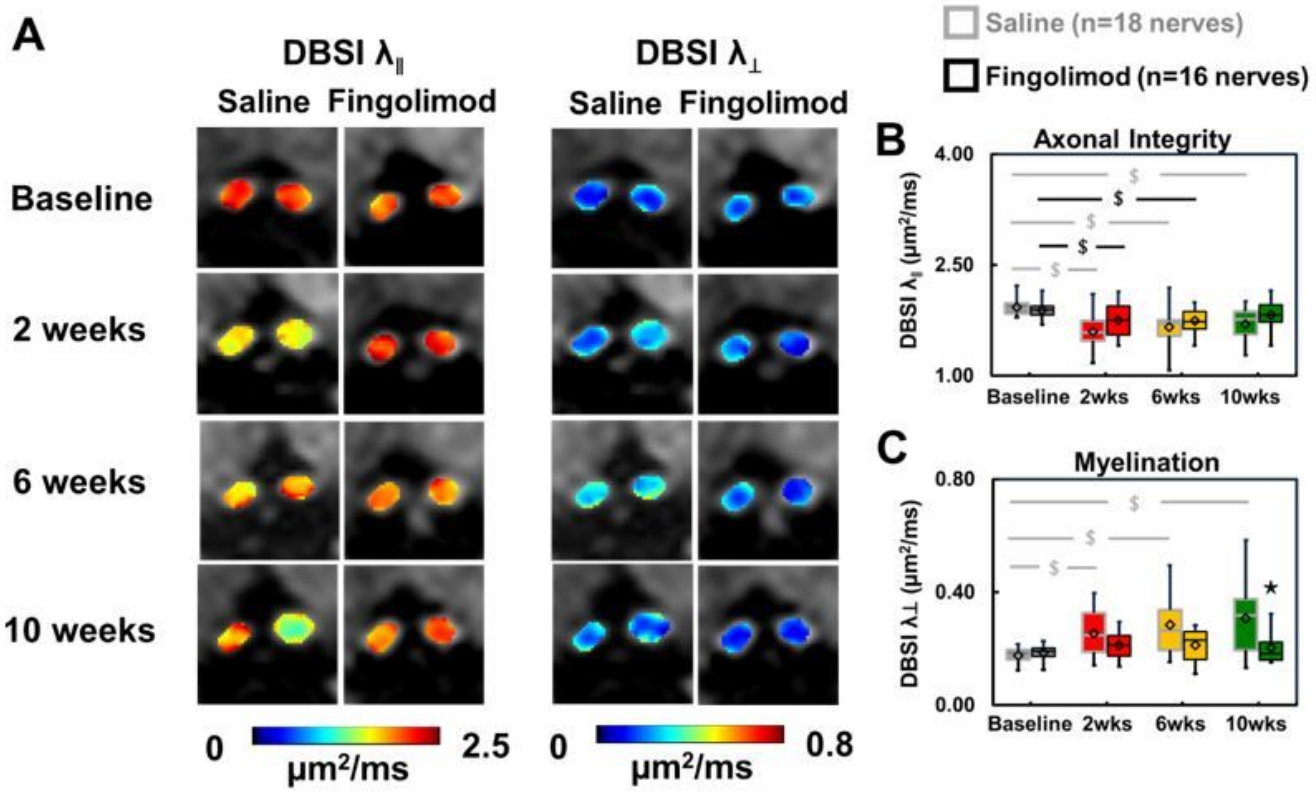

Figure 4

DBSI-derived axial (λ∥) and radial (λ⊥) diffusivity maps of representative saline- and Fingolimod-treated optic nerves from baseline to 10-week treatment (A) were derived from anisotropic diffusion tensor components. Comparing to baseline, significantly decreased DBSI-λ∥ was detected at all time points in saline-treated optic nerves (B, $p < 0.05$). In contrast, decreased DBSI- λ∥ was only seen at 2 and 6 weeks in Fingolimod-treated optic nerves (B, $p < 0.05$). Significantly increased DBSI-λ⊥ was detected in saline-treated ($p < 0.05$) but not in Fingolimod-treated optic nerves at all time points (C). The results showed intermittent axonal injury during Fingolimod treatment. After 10-week Fingolimod treatment, DBSI-λ∥ and DBSI-λ⊥ were not different from their baseline values (B, C). ⋆ indicates $p < 0.05$, comparing between saline and fingolimod groups $ indicates $p <0.05$, comparing to its baseline within group

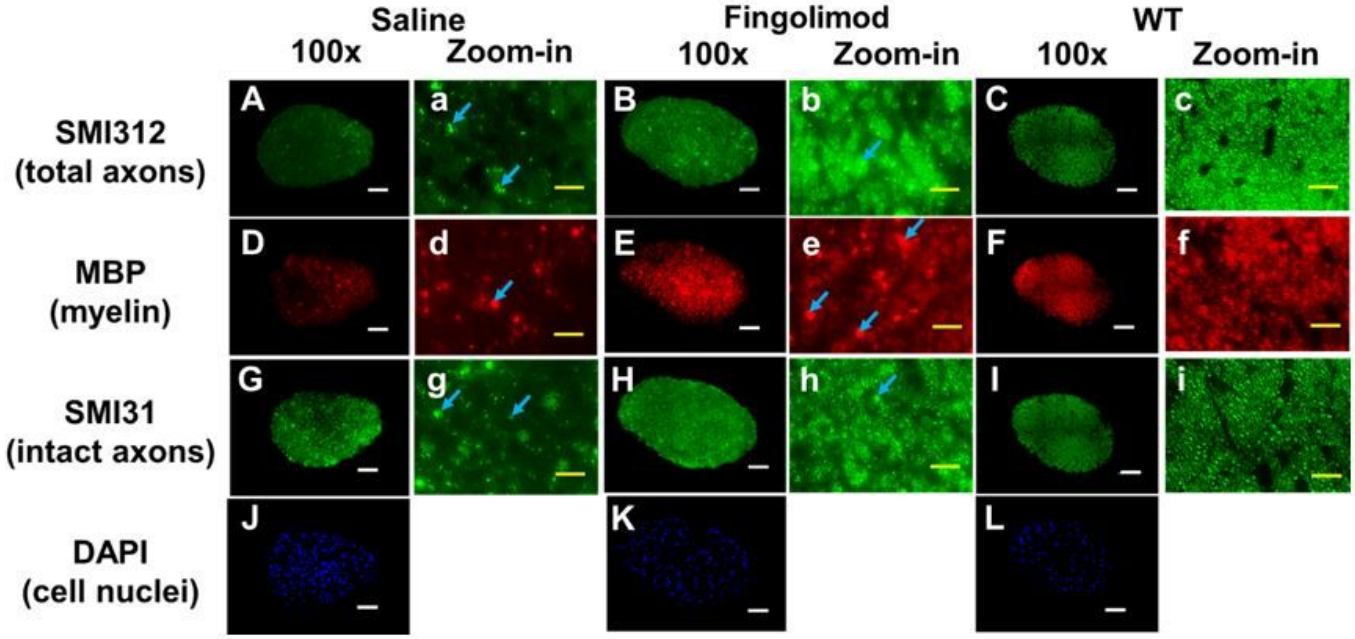

Figure 5

Representative 100× immunohistochemical staining images of total neurofilament (SMI-312, staining both injured and intact axons, A–C), myelin basic protein (MBP, assessing myelin, D–E), phosphorylated neurofilament (SMI-31, reflecting intact axons, G–I), and 4', 6-dianidino-2-phenylindole (DAPI, detecting nuclei, J – L) from saline-, and Fingolimod-treated optic nerves at 10 weeks after treatment. Comparing to wild-type (WT) optic nerves, saline-treated optic nerves showed lowest staining intensity in SMI-312 (A), MBP (D), and SMI-31(G), suggesting axonal loss, demyelination, and axonal injury, respectively. Regarding Fingolimod-treated optic nerves, moderate lower staining intensity in SMI-312 (B), MBP (E), and SMI-31(H), suggesting mild axon and myelin injury were assessed. Blue arrows indicated swelling axon and myelin. Strongest DAPI stains in saline-treated optic nerve (J) suggested highest cellularity than Fingolimod-treated (K) and wild-type (L) optic nerves. White scale bar: 50 μm Yellow scale bar: 10 μm

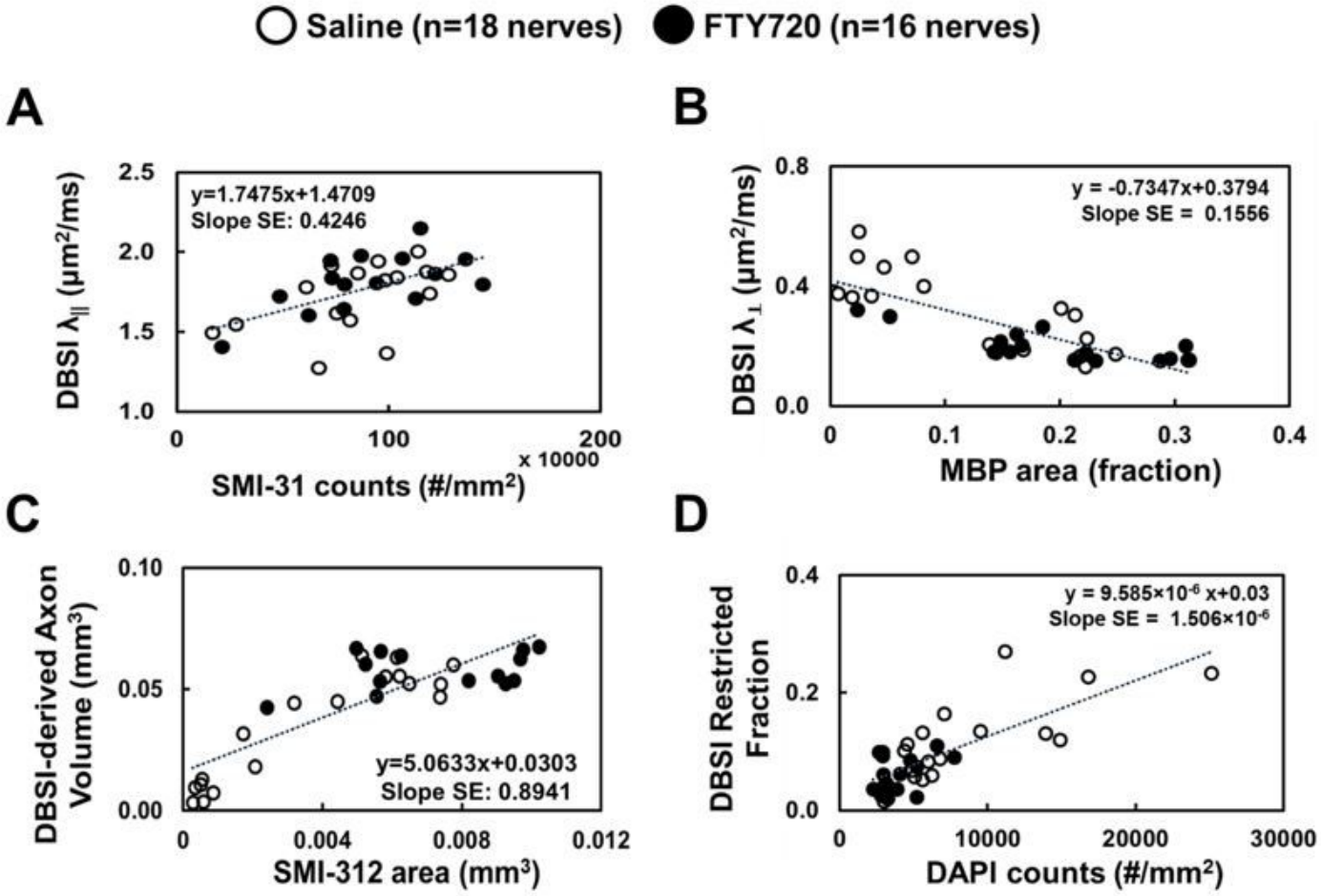

Figure 6

Mixed random-effect regression analysis for the correlation between DBSI parameters and IHC biomarkers. SMI-31 counts and MBP area fraction (the ratio of positive staining counts and total tissue area), SMI-312 area (absolute value of positive staining counts), and DAPI counts were statistically significant associated with DBSI-λ∥ (A), DBSI-λ⊥(B), DBSI-derived axonal volume (C), and DBSI restricted isotropic fraction (D), suggesting that in vivo DBSI quantitatively reflected the complicated pathologies including axonal injury, demyelination, axonal loss, and cell infiltration.